ION SOURCES

N. Angert
GSI, Darmstadt, Germany

Abstract
In the first part fundamental principles of positive and negative ion production are presented. Then a selection of positive ion source types is described which are relevant for accelerator application, beginning with low-charge-state high-current sources up to highly-charged ion sources. This is followed by a brief review of negative ion sources, and finally some basic remarks on beam extraction and formation.

1. INTRODUCTION

Ion sources have uses in a variety of research fields and applications such as mass separation, ion implantation, fusion, space propulsion, atomic physics and in accelerators for nuclear and particle physics. The large proton accelerator facilities for particle physics need beams of hundreds of mA, but intense H^- are very attractive, too. Tandem accelerators also start with negative ions of hydrogen to produce heavy ions stripped to high charge states at high potential. During the last decade there has been an increasing interest in medium- and high-energy, heavy-ion beams ranging from several MeV/u to some 100 GeV/u. The design of injector accelerators for this application is strongly influenced by the charge states and intensities which can be delivered from the heavy-ion sources.

This paper cannot deal with all the different types of ion sources used, but it will try to give an idea of their variety and will explain the principles of the most important ones from the author's point of view, which is somewhat influenced by heavy-ion accelerators.

2. PRINCIPLES

2.1. Production of Positive Ions

Positive ions can be created by using photons, electrons or surface-contact ionization to supply the ionization energy. Here only ion sources are discussed in which bombarding electrons are used. The basic process is

$$e + X \rightarrow X^{+} + 2e \qquad (1)$$

or for multipli-charged ions

$$e + X^{i+} \rightarrow X^{(i+1)+} + 2e \qquad (2)$$

assuming only outer-shell step ionization and neglecting e.g. Auger processes etc.

Figure 1 shows the ionization energies vs nuclear charge for different ionization states. In Figure 2 the ionization cross sections vs bombarding electron energy are shown for different charge states of argon. It can be seen that, after a steep increase, the cross section for a certain charge state reaches its maximum at about three times the ionization potential, and decreases slowly with increasing energy of the bombarding electron. It decreases with increasing charge state. For high production cross section of a charge state, the electron energy should be about three times the ionization potential; that means 10 to 40 eV for singly-charged ions, several hundred eV for multipli-charged states and keV to tens of keV for highly-charged ions.

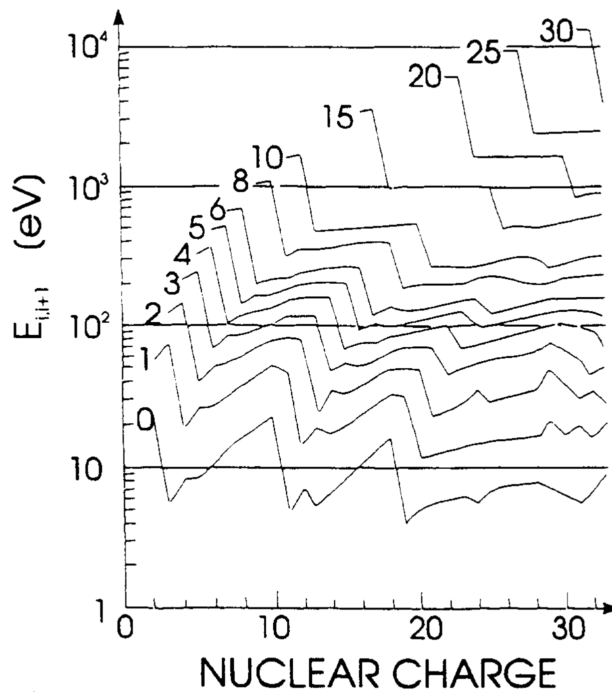

Fig. 1 Ionization energies for step-by-step ionization of elements up to nuclear charge 30

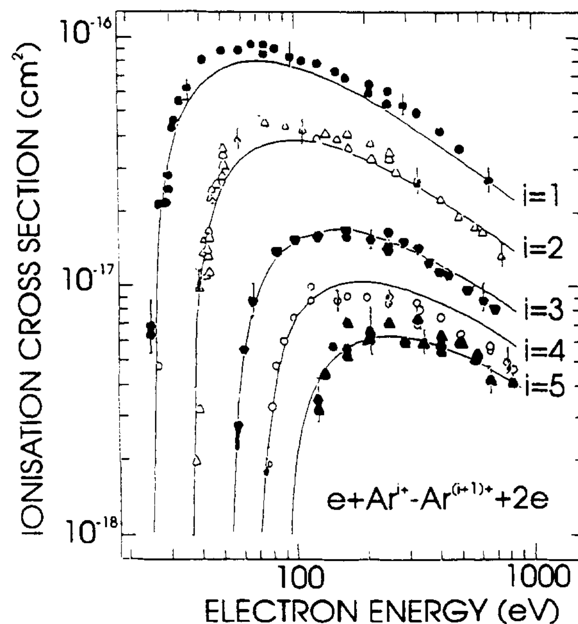

Fig. 2 Ionization cross-section versus bombarding electron energy for different charge states

The time necessary for an atom to reach a certain charge state depends on the cross section and the electron current density. In competition with the ionization are the loss processes, diffusion out of the ionization volume or charge exchange processes with neutral atoms. Taking this into account the time evolution of the charge state distribution can be calculated from the following simplified differential equation [1]

$$dn_0 / dt = n_0 \sigma_{0,1} j_e \tag{3a}$$

and

$$dn_i / dt = n_{i-1} \sigma_{i-1,i} j_e - n_i \sigma_{i,i+1} j_e - n_i / \tau_c(i) \tag{3b}$$

where:

n_0 is the neutral particle density

n_i is the ion density in charge state i

$\sigma_{i-1,i}$ is the cross section for single step ionization into charge state i

j_e is the electron current density

$\tau_c(i)$ is the life time of ion in charge state i (containment time) without ionization

The charge state distribution is mainly determined by σ, i.e. by the energy of the electrons, and $j_e \tau_c$, the product of electron current density and containment time. The diffusion time out of the ionization volume without any confinement is in the range of μs. By special magnetic and electric fields containment times up to s can be achieved if charge exchange is negligible. The dominant charge exchange process is with neutral atoms. The charge exchange between ions is much smaller because of Coulomb repulsion. The life-time is in the range of tens of ms for a residual gas pressure in the range of 10^{-6}—10^{-7} torr [2]. From Eq. (3) one can draw the following conclusions:

a) high j_e and n_o lead to high current, but not to high charge states because of short τ_c

b) high electron energy, low pressure and long containment is needed for high charge states.

This leads to the schematic diagram shown in Figure 3, where $n_e \tau_c = j_e \tau_c / v_e$, ($v_e$ electron velocity) is taken for the abscissa. $n_e \tau_c$ is a figure of merit as used in fusion reactors.

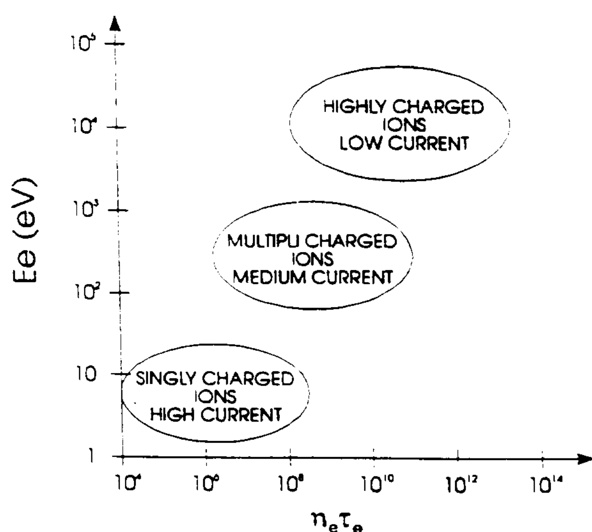

Fig. 3 Operating parameters for different types of ion sources. Electron energy vs. electron density times containment time.

2.2. Production of Negative Ions

The processes involved in the attachment of an electron to a neutral atom are exothermic in contrast to the endothermic processes required for positive-ion formation. The binding energy or electron affinity E_A of the negative-ion is a measure of the stability and ease of ion formation. Table 1 displays atomic electron affinities [3]. E_A must be positive for negative-ion stability. Negative values refer to unstable negative-ion states. In addition to negative-atomic-species formation, many molecular negative ions have been observed. There is also an important class of negative ions which are only formed in excited metastable states.

Negative ions may be formed by means of several physical or physico-chemical mechanisms such as volume processes by electron impact, charge-exchange in metal vapours and on surfaces. Compared to positive-ion production there is a large variety of possible processes. Only a few can be considered here.

2.2.1. Processes in Volume [4]:

Dissociative Attachment: Slow electrons are stably attached to atoms during their interactions with neutral molecules preferentially with excited ones according to the following reaction

$$e + XY \rightarrow X^- + Y \tag{4}$$

Polar Dissociative Attachment: In this case the electron is not captured but only excites the molecule to an unstable state

$$e + XY \rightarrow X^+ + Y^- \tag{5}$$

Table 1

Electron affinities and ionization energies of elements

Group: Ionization potential (eV) -- Electron affinity (eV)

I A	II A	III A	IV A	V A	VI A	VII A	VIII A
1 H 13.59 0.75							2 He 24.58 0.078
3 Li 3.39 0.62	4 Be 9.32 < 0	5 B 8.30 0.28	6 C 11.26 1.26	7 N 14.54 ≤ 0	8 O 13.61 1.46	9 F 17.42 3.39	10 Ne 21.56 < 0
11 Na 5.14 0.54	12 Mg 7.64 < 0	13 Al 5.98 0.46	14 Si 8.15 1.38	15 P 10.55 0.74	16 S 10.36 2.07	17 Cl 13.01 3.61	18 Ar 15.76 < 0
19 K 4.34 0.50	20 Ca 6.11 ≈ 0	31 Ga 6.00 0.3	32 Ge 7.88 1.2	33 As 9.81 0.80	34 Se 9.75 2.02	35 Br 11.84 3.36	36 Kr 14.00 < 0
37 Rb 4.18 0.48	38 Sr 5.69 < 0	49 In 5.78 0.3	50 Sn 7.34 1.25	51 Sb 8.64 1.05	52 Te 9.01 1.97	53 I 10.45 3.06	54 Xe 12.13 < 0
55 Cs 3.89 0.47	56 Ba 5.21 < 0	81 Tl 6.11 0.3	82 Pb 7.41 1.1	83 Bi 7.29 1.1	84 Po 8.43 1.9	85 Ar 9.5 2.8	86 Rn 10.74 < 0

III B	IV B	V B	VI B	VII B	VIII B	VIII B	VIII B	I B	II B
21 Sc 6.56 < 0	22 Ti 6.83 0.2	23 V 6.74 0.5	24 Cr 6.76 0.66	25 Mn 7.43 < 0	26 Fe 7.90 0.25	27 Co 7.86 0.7	28 Ni 7.63 1.15	29 Cu 7.72 1.22	30 Zn 9.39 < 0
39 Y 6.5 = 0	40 Zr 6.95 0.5	41 Nb 6.77 1.0	42 Mo 7.18 1.0	43 Tc 7.28 0.7	44 Ru 7.36 1.1	45 Rh 7.46 1.2	46 Pd 8.33 0.6	47 Ag 7.57 1.303	48 Cd 8.99 < 0
57 La 5.61 0.5	72 Hf 7.0 < 0	73 Ta 7.88 0.6	74 W 7.98 0.6	75 Re 7.87 0.15	76 Os 8.7 1.1	77 Ir 9.0 1.6	78 Pt 8.96 2.12	79 Au 9.22 2.30	80 Hg 10.43 < 0

Dissociative Recombination [5]: By collisions of slow electrons with positive molecular ions, negative ions are generated with considerable cross section by the following reaction

$$e + XY^{+} \rightarrow X^{+} + Y^{-} \quad (6)$$

2.2.2. Charge exchange processes in metal vapour [6]:

In charge-exchange processes in alkali or alkaline-earth vapour targets a fraction of a positive-ion beam can be converted into negative ions. The conversion efficiency ranges from 0.5 to > 90 % [7,8]. This mechanism offers a practical and efficient means of producing useful beams from elements which have positive electron affinity.

2.2.3. Processes on surfaces [9]:

Interaction between particles having sufficient energy and a low work function surface can result in the formation of a negative ion. This effect can be enhanced with alkali coatings at the surfaces exposed to the bombardments. There are two principle processes, namely the thermodynamic-equilibrium surface ionization, where the slow atom or molecule impinging on the surface is emitted as a positive or negative ion after a mean residence time, and the non-thermodynamic atom-surface interaction, where negative ions are produced by sputtering a material in the presence of an alkali metal coating [10].

3. ION SOURCES FOR POSITIVE IONS

3.1. High-Current Ion Sources

3.1.1. Filament ion sources

In its simplest form a high-current ion source consists of a cathode filament surrounded by an anode cylinder or cube and an aperture in the extraction plate opposite the cathode (Fig. 4). The end plates E1 and E2 can be at anode, floating or near cathode potential to reflect the electrons to provide a higher ionization efficiency.

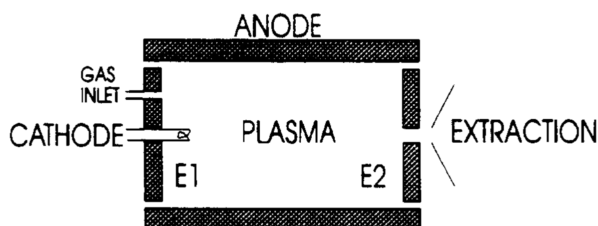

Fig. 4 Schematic of a high current source. Endplates E1, E2 can be part of the anode, floating or near cathode potential

Discharge is ignited at a gas pressure of 10^{-1} to 10^{-3} torr. Such a device needs a high discharge current because of the large anode area. With the availability of strong permanent magnets multi-cusp devices are more and more used to create the plasma needed in high-current sources for singly-charged ions. The discharge vessel is surrounded by magnets with alternating polarity, creating a minimum-B configuration which reduces the effective anode area and yields a quiet, homogeneous plasma of large cross-sectional area. Figure 5 shows a cubic multi-cusp source [11]. A cylindrical version of the reflex type is shown in Figure 6 with its multipole-field configuration. This source was especially developed for singly-charged, high-current, heavy-ion beams of up to 100 mA operating with discharge voltages and currents of 10—100 V and 20—150 A, respectively. For further high current sources the reader is referred to ref. [12,13]

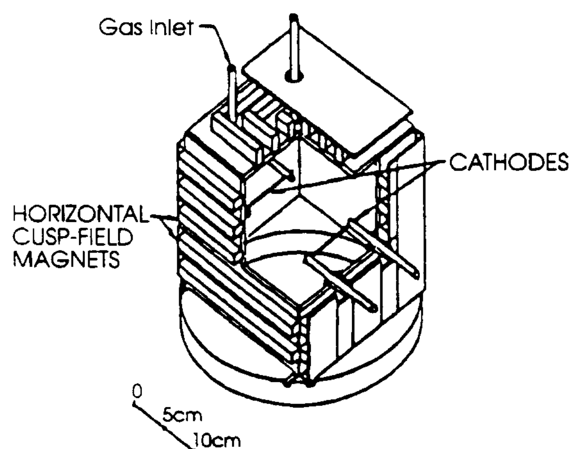

Fig. 5 Multicusp ion source. Ions are extracted towards the bottom.

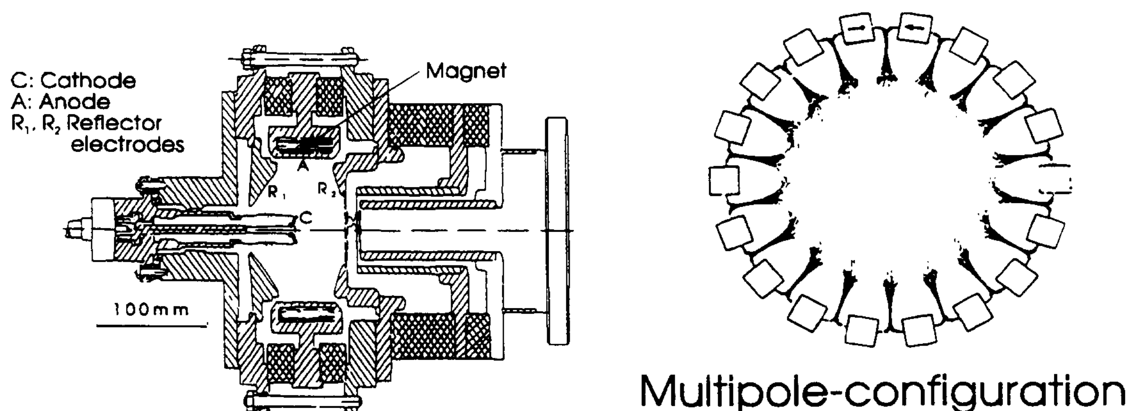

Fig. 6 Multicusp ion source for heavy ions

3.1.2. Microwave ion sources

Dense plasmas can also be generated by an rf discharge [14] or microwave discharge in a magnetic field [15]. In this way filament break down and replacement is avoided. Microwave sources can be classified into two types. One is operated at the electron cyclotron resonance (ECR) to obtain, in a low pressure regime, multipli-charged ions as described in a later chapter. The other uses off-resonance microwave plasma in the 10^{-3} to 10^{-1} torr range to obtain high currents of singly-charged ions [16]. The extractable ion-current density is proportional to the product of electron density n_e and the square root of the electron temperature T_e. These parameters can be raised by increasing the absorbed microwave power. Microwave ion sources provide ion beams of higher current and smaller energy dispersion than rf ion sources since ions in the plasma are not accelerated by a microwave electric field as they may be in an rf electric field.

Microwaves (typically 2.45 GHz) can be introduced into the discharge chamber either via a coaxial line or a microwave window from a rectangular wave guide. An

example of this design, which has been used in recent years, is shown in Figure 7 [17]. Total beam currents of oxygen ions of up to 270 mA 0^+ have been obtained from an extraction area of 3.7 cm². Microwave ion sources should be especially suited to high-current cw operation. A typical application is described in Ref. [18].

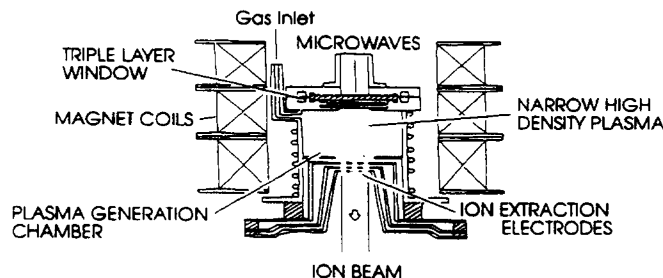

Fig. 7 Microwave ion source

3.1.3. Metal vapor vacuum arc (MEVVA) ion source

The high-current ion sources described above are especially suited for operation with gases or gaseous compounds. Nevertheless beams of up to several tens of mA of metal ions have been reached for some species [e.g. 12].

During the last few years MEVVA-type ion sources have been developed for high-current ion beams for a wide range of solid materials [19,20]. In this ion source a metal vacuum arc is used to generate the plasma from which the ions are extracted. The source is mostly for pulsed beams, but dc operation development is proceeding, too [21].

3.2. Multipli-Charged Ion Sources

3.2.1. Duoplasmatron

An ion source which has been in use for many years, both for the production of high-current proton beams and low-charged, positive heavy ions, is the duoplasmatron source [22] (see Fig. 8). The discharge plasma is sustained by a thermionic cathode and radially compressed by means of an intermediate electrode and an axial magnetic field. The anode and the intermediate electrode are made from ferromagnetic material and form the pole pieces of a magnetic yoke. Due to the constrictions of the discharge, one or more double layers are generated along the plasma column, separating regions of different neutral pressure and plasma density. Near the anode there exists a relatively dense plasma with a high degree of ionization, whose potential is higher than that the anode [23]. The ions are extracted through a small outlet aperture in the anode. Typical discharge voltages and currents for multipli-charged ion production are up to 250 V and 20 A, respectively. This results in electron-current densities j_e of more than 100 A/cm². The residual gas pressure is about 10^{-2}—10^{-3} torr. However, the containment time is only µs. Therefore the maximum charge states obtained are ≤ 10+ for e.g. xenon with µA intensities [24].

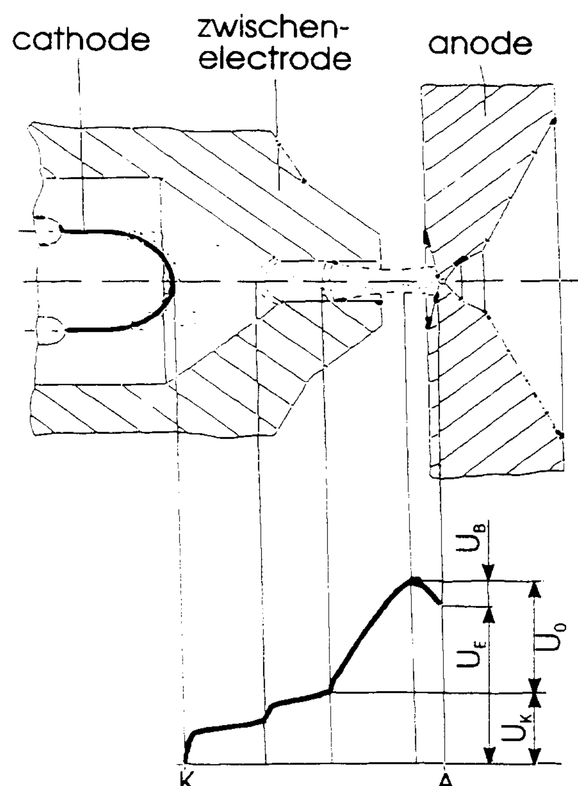

Fig. 8 Discharge region of duoplasmatron and potential along discharge

3.2.2. PIG (Penning ion gauge) source

Figure 9 shows the principle of a PIG source for multipli-charged ions. It consists of the two cathode blocks and a cylindrical anode in a magnetic field parallel to the anode axis. Contrary to the duoplasmatron source, where the electrons pass only once from the cathode to the anode, in the PIG source electrons are emitted from one cathode, follow the B-field lines to the other cathode, and are reflected there. They oscillate in this way a few times through the discharge thereby increasing the electron current density. Ions can be extracted either axially, through a hole in one cathode or, as is commonly done, radially through a slit in the anode, using the magnetic field simultaneously for charge analysis.

To get the maximum value for the total ionization cross section and hence the maximum production rate for the ions, the electron energy must be about three to five times the ionization energy for step-by-step ionization of the charge state considered. Therefore, it is advantageous to control the arc impedance and hence the electron energy. This is achieved by applying additional heat to one cathode by an electron current from a filament. The output is then optimized by proper choice of arc-current, cathode-heating, and gas-flow, which corresponds to neutral density. These parameters influence the electron density, electron energy, and charge-exchange losses. Figure 10 shows the PIG source design used at the UNILAC. The top cathode is heated by electron bombardment, whereas the so-called anti-cathode is cooled. Solid materials can be fed into the discharge by sputtering from an electrode negatively biased with respect to the anode. This source type has been adopted from Orsay [25] and is based on the Dubna design [26,27]. The output of the PIG source is

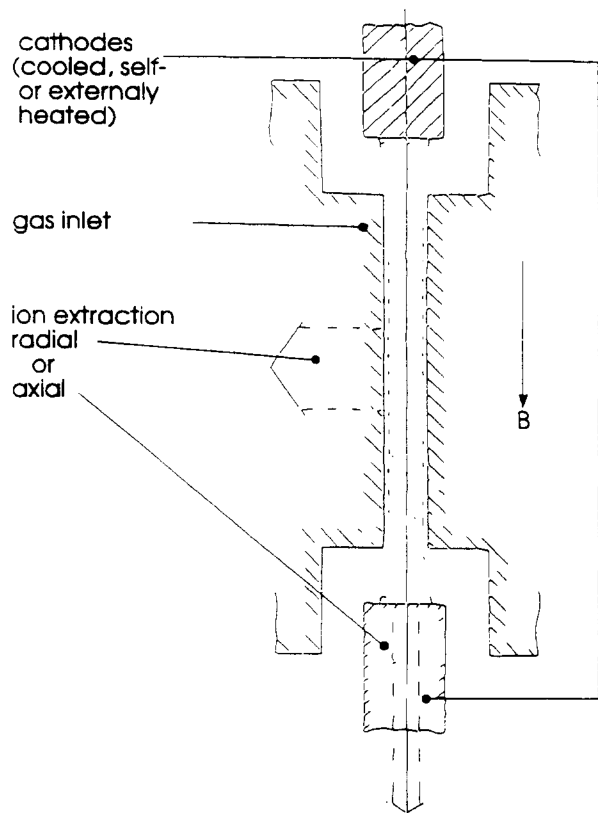

Fig. 9 Schematic of PIG source

about 100 times higher than from a duoplasmatron for charge states 7+ to 10+. Intensities of 50 to 100 μA are routinely achieved for charge states 9+ or 10+ of Au, Bi and U within a normalised emittance of 0.5 π mm mr at the GSI UNILAC. Typical discharge voltages and currents are in the range up to 2000 V and 10 A. The residual gas pressure is estimated to be about 10^{-4} to 10^{-3} torr.

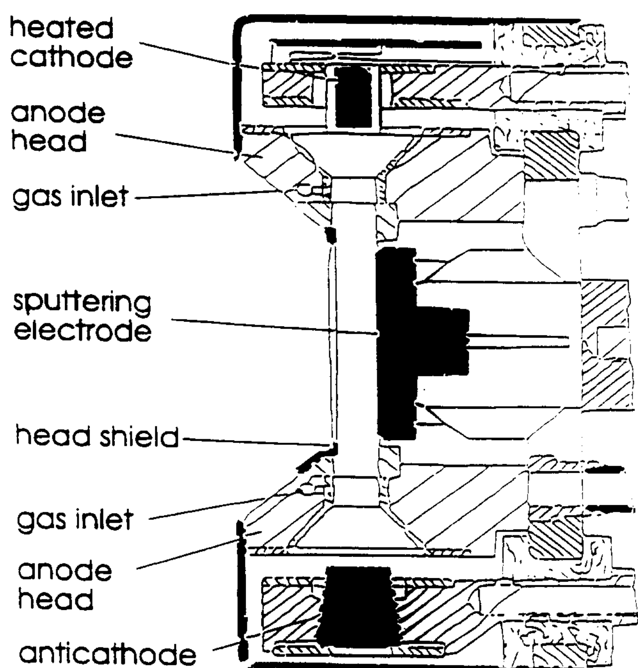

Fig. 10 GSI PIG source

3.3. Highly-Charged Ion Sources

3.3.1. Electron-beam ion source (EBIS)

In an EBIS (see Fig. 11) an external electron gun launches a small diameter electron beam into the ionization volume containing atoms of the desired element down the axis of a solenoid [28]. The beam stops on the electron collector in the magnetic stray field. The potential along the axis is defined by a number of cylindrical drift tubes. During a short "injection" period, the desired number of ions is accumulated in the well. The ions are contained radially in the electrostatic potential well of the electron beam and axially by the potential barriers on the end drift tubes. Then the potential distribution is switched to the "ionization" mode, in which the first barrier is moved downstream (see Fig. 11) to prevent additional low-charge-state ions from entering the containment volume. When the average charge state has reached the desired value, the potentials are switched to the "extraction" mode. This applies a potential ramp accelerating the ions into the extractor. Typical extraction times are about 50 μs, at 1—10^3 Hz repetition rate.

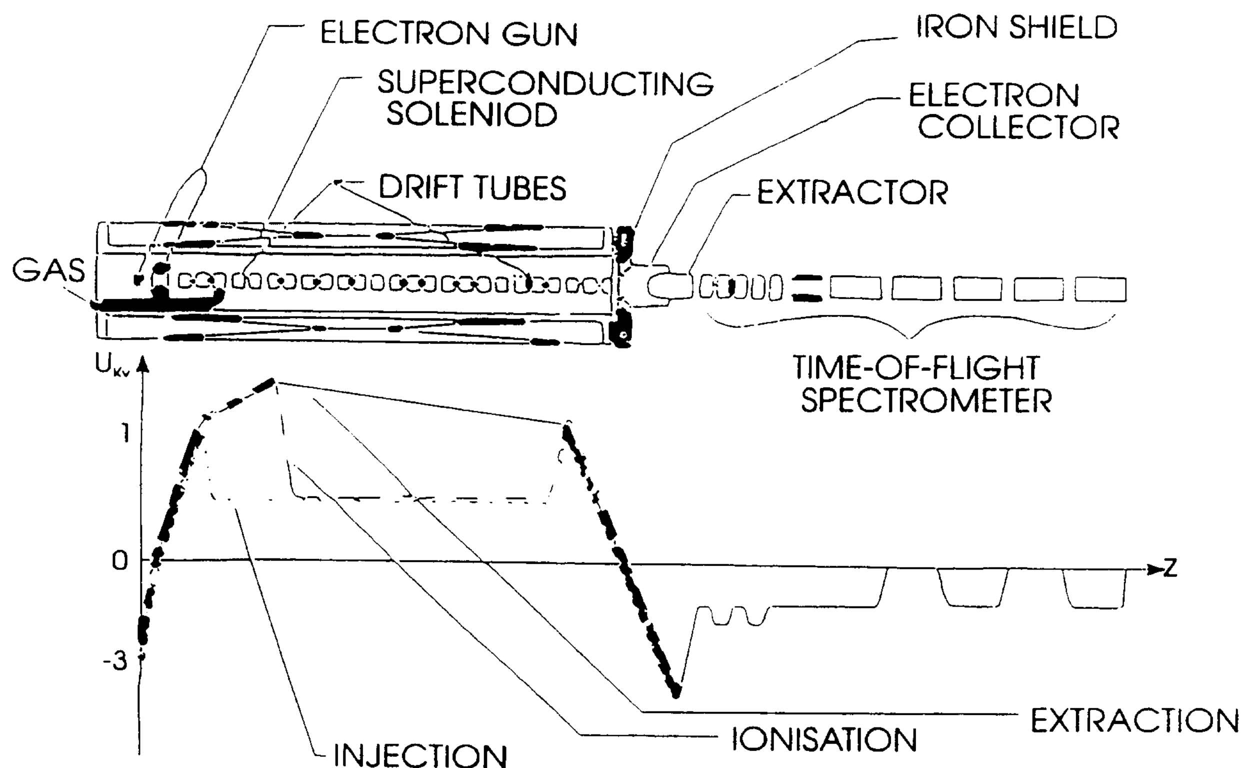

Fig. 11 Schematic drawing of Krion EBIS source potential distribution for different operating steps

The EBIS source is almost ideal for very high charge states. Commonly operated at very low residual gas pressures down to 10^{-10} torr, and based on very good radial and axial confinement, containment times up to seconds can be achieved. In addition, high electron energies can be applied. Figure 12 shows a calculated evolution of charge-state population with the product $j_e\tau_c$ for Ar with a 10 keV electron beam [29]. For a 10 keV, 1 A electron

beam and 1 m containment length, the theoretical number of ions which can be accumulated is $10^{11}/i$, where i is the average charge state. Actual sources achieve about 10 % of the theoretical values [30]. In addition to the "injection" mode described above, ion injection from an external source (see Fig. 13), which also allows the use of solid material elements, has been successfully tested [31]. Most EBIS sources have superconducting solenoids [28,30,32,33].

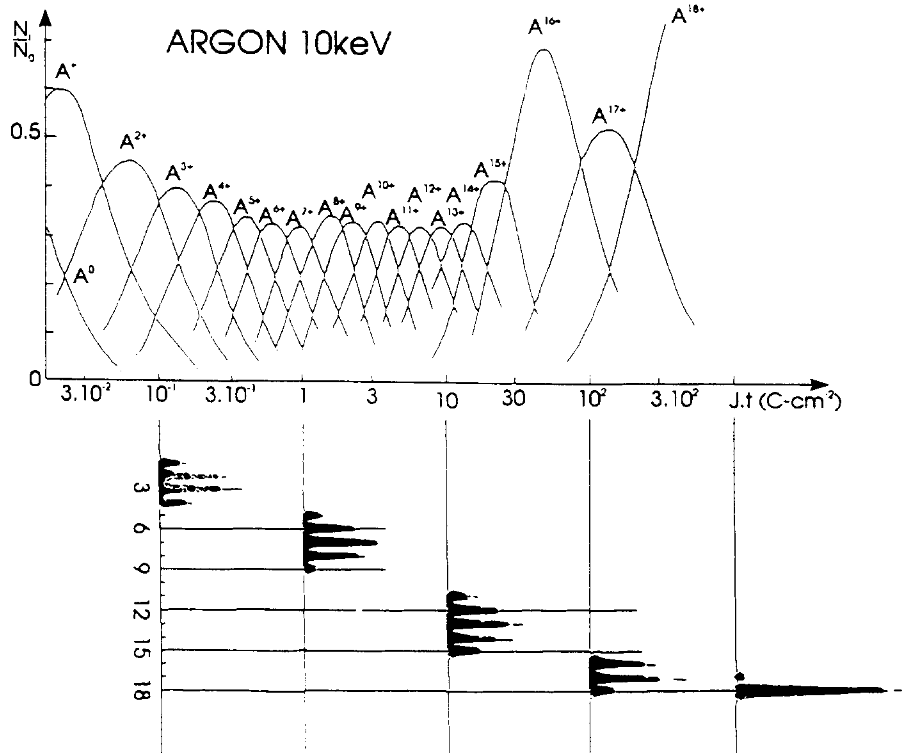

Fig. 12 Calulated evolution of charge state distribution for argon with product $j\tau$ with a 10 keV electron beam

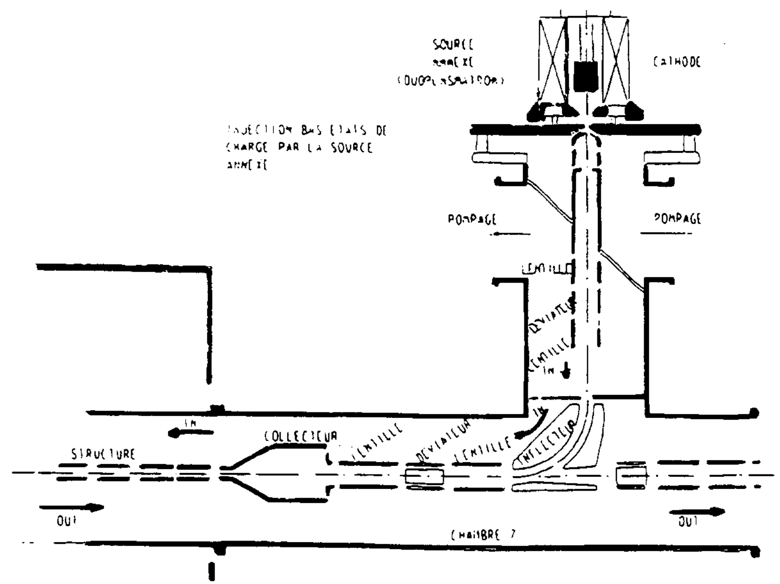

Fig. 13 Saclay external ion injection into EBIS source

In recent years confinement times of ions as well as the charge states achieved in the EBIS devices have been considerably increased. However, due to beam-plasma instabilities there is still a limitation in the number of charges that can be collected in this source type. For light ions it is 10^{11}, and about an order of magnitude less for heavy ions [34]. An additional loss of heavy ions is caused by the ionization process during the confinement which heats the ions so that they can leave the trap potential. By the addition of light atoms such as He, energy is transfered by Coulomb collisions to the light species which can more easily escape due to the lower charge state. Thereby the heavy ions are "cooled" and their confinement time is increased. Thus the yield of high charge states of Kr could be considerably increased [35]. The same cooling process by light ions seems to support the generation of high charge states in the ECR ion source described in the following section.

3.3.2. Electron-cyclotron-resonance (ECR) ion source

In an ECR source the ionizing electrons do not gain the desired energies in a plasma sheath or by electrostatic acceleration from a cathode, but the electrons of the plasma itself are accelerated by an oscillating electromagnetic wave [29]. If a metallic box (see Fig. 14) is filled with microwave power (e.g. f = 10 GHz, λ = 3 cm) the box can be considered as a multimode cavity, if it is large with respect to λ. If this box is put into a minimum-B structure where the magnetic field strength is between 0.2 and 0.5 T, there must be a magnetic surface where the field strength is B_0 = 0.36 T and the gyrofrequency of the electrons 10 GHz. Such a surface creates an electron cyclotron resonance, as there is always a component of the electric field perpendicular to the magnetic field in a multimode cavity. If the electrons pass many times through this surface, they are stochastically heated.

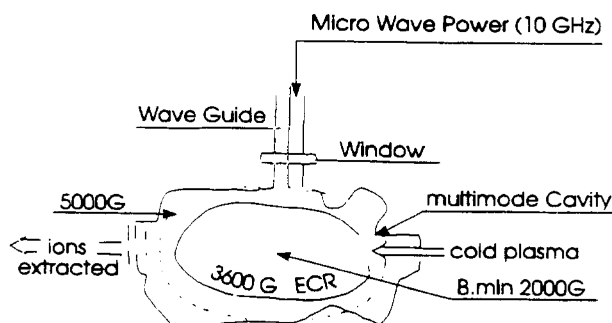

Fig. 14 Schematic of the ECR ion source

Figure 15 shows the two stage MICROMAFIOS source of Geller built in 1979. A plasma is produced in the first stage at high pressure (10^{-2}—10^{-3} torr) by microwave power in an axial magnetic field. From there the cold plasma diffuses into the second stage. Here the ionization to high charge states is done by energetic electrons of up to several ten keV created by the ECR process. The background pressure in this stage must be $< 10^{-6}$ torr to prevent charge-exchange losses. For a long confinement time of the ions, a radial sextupole field is superimposed on the axial mirror configuration of the second stage, in a minimum-B configuration. A modified version of this type, the so called MINIMAFIOS source was used at the accelerators in Grenoble, Caen and CERN already in the mid-eighties. It was operated both in cw and pulsed mode. The latter offered three to five times enhanced yield for high charge states of light ions. For instance 100 μA 0^{6+} could be achieved in this mode.

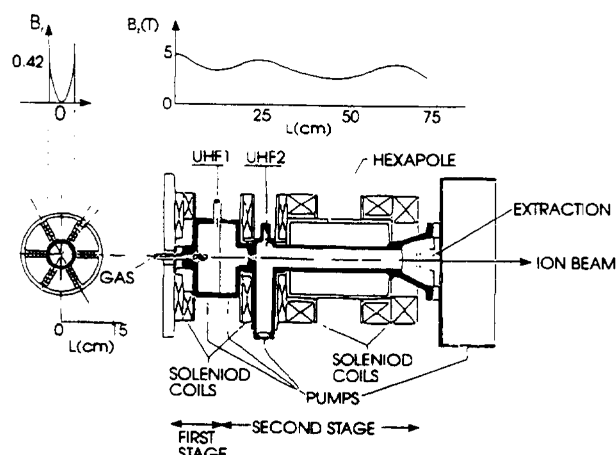

Fig. 15 The two stage MICROMAFIOS ECR source of Geller.

In the first sources, operated at 10 GHz microwave frequency, Sm-Co permanent magnets were used to build the sextupole for radial confinement. With the availability of Nd-Fe-B permanent magnets resonance fields of 0.51 T instead of 0.36 T became possible. This leads to a cyclotron resonance frequency f of 14.5 GHz (this is a satellite communication frequency so that transmitters are available) instead of 10 GHz and consequently double the plasma density n_e, because the critical propagation frequency in a plasma is proportinal to n_e^2. Today some 40 ECR ions sources are in use round the globe. Most of them are in use at cyclotrons as the cw mode makes it an attractive source for this type of accelerator, because it has no filaments or cathodes. In addition it can deliver higher charge states than e.g. the PIG sources what leads to higher output energies ($E = Kq^2/A$, q = charge state, A = atomic mass) for a given K-value of a cyclotron. For further information the reader is referred to Ref. [36].

During the last few years considerable progress has been made in the development for high-charge-state very-heavy ions. Examples are given in references [37] and [38] for cw operation, indicating that about 10 μA in charge state 25+ are achievable for Au, Bi and U ions.

Besides the cw and pulsed operation mode there exists a third mode, the so-called "afterglow" mode in which an ECR ion source can be run. It was first observed on the MINIMAFIOS 16-GHz source in Grenoble in 1988, that after the rf power was turned off the extracted ion current showed for a about 500 μs, a sharp increase in intensity [39]. The source design and operation parameters to optimize the ion output have been improved in the last years. Today 100 μA of Pb^{28+} are achieved [40]. Figure 16 shows the GANIL ion source ECR 4 (14.5 GHz) developed for this kind of operation. It can be seen that, today, ECR ion sources have an iron core to reduce both the size and power consumption of the magnet field. Usually present-day ion sources have one common rf supply for their first and second stage.

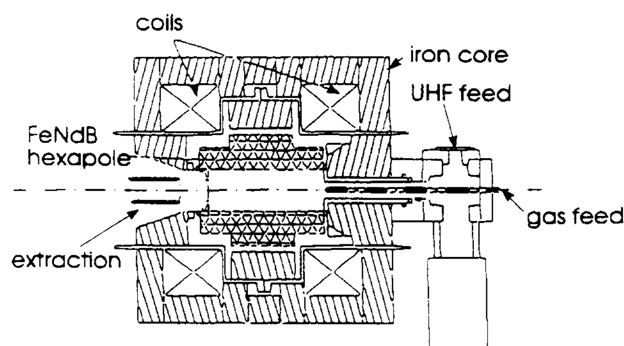

Fig. 16 The GANIL ion source ECR4.

3.3.3. Laser ion source

The possibility to extract highly-charged ions from laser-beam-induced plasma has been investigated for many years. However, application to accelerators has been tried only in a few cases [41]. Multipli-charged ions could be produced up to charge states of about 10 to 15+ with resonable yield. With the availability of CO_2 lasers with rather high peak power new attempts have been started at several places to produce highly-charged ions for accelerator application [42,43]. Charge states of up to 26+ for lead have been observed on a new test bench at CERN.

4. ION SOURCES FOR NEGATIVE IONS

4.1. Volume Produced Negative Ion Sources

4.1.1. "Classical" negative ion soources

H^- ions are very important nowadays both for injection in circular accelerators, where by stripping to H^+ the injection is not limited by Liouville's theorem, and for H^0 injection in fusion devices. About twenty years ago, most H^- sources were adapted positive-ion sources such as duoplasmatrons, Penning sources and magnetrons [44,45].

Figure 17 shows a schematic of a magnetron source. In a magnetic field of 1—2 kG a discharge is established between a cold cathode and an anode mounted in such a way that there are closed E x B loops around the cathode. Electrons emitted from the cathode by secondary and photoelectric emission are accelerated towards the anode and bent by the magnetic field, describing cylindrical trajectories around the cathode. Most existing magnetron sources incorporate two substantial improvements: the cathode surface opposite the extraction slit has the shape of a cylindrical groove so that the H^- ions produced are focused into the extraction slit; second the gap between the cathode and the anode is not uniform [46]. By that measure current densities up to 3 A/cm² could be achieved.

4.1.2. Multi-cusp negative ion sources

As described in section 3.1 multi-cusp plasma generators are suited to produce large volume of quiescent and uniform plasmas. Figure 18 shows a H^- source developed by Leung et.al at LBL [47]. It looks like a positive ion high-current source, but when operated

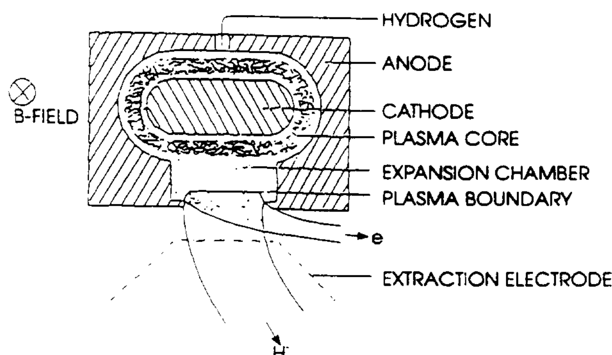

Fig. 17 Schematic drawing of a magnetron source.

as a H^- source a water-cooled magnet filter is included. This filter provides a transverse magnetic field near the extraction zone, which is strong enough to prevent the energetic primary electrons from the cathode from entering the extraction zone. Both positive and negative ions, together with very slow electrons, are able to penetrate the filter and to form a cold plasma in which H^- ions can be produced by volume processes with high efficiency.

The same scheme can be used by replacing the filament by an rf-antenna (Fig. 19) for plasma generation [48]. Thereby the source can be operated without short life components and could also be used for reactive gases which would poison a filament. Volume processes are especially suited for generation of negative ions from gases, gaseous compounds or vapours. For solid materials other types of negative ion sources are in use to be described in the following sections.

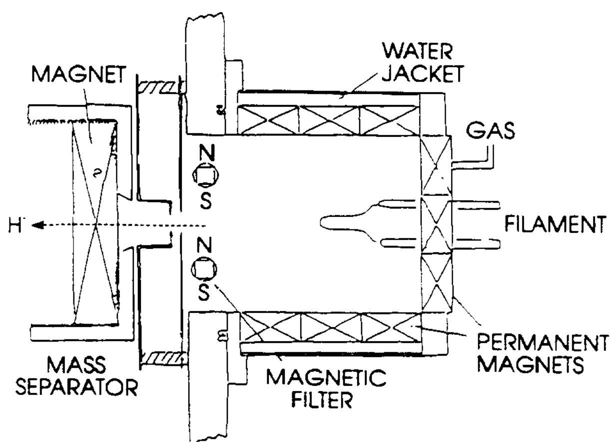

Fig. 18 LBL negative ion source with filament.

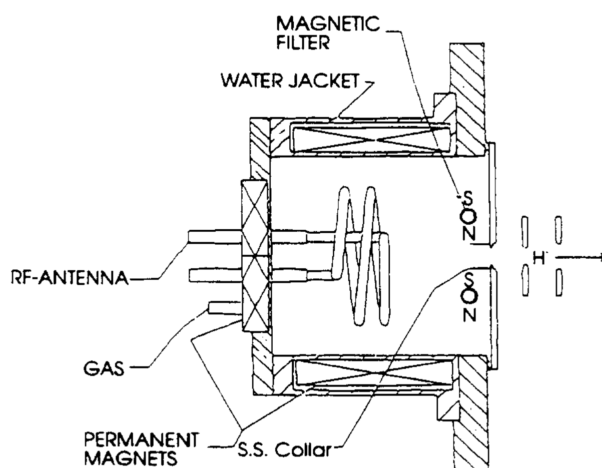

Fig. 19 LBL negative ion source with rf plasma generation.

4.2. Charge-Exchange Sources

Sources of this type consist of a positive-ion source for singly-charged ions and a charge-exchange canal where the exchange interactions take place. The exchange canal is usually a tube 0.75 cm in diameter and $\approx$ 5 cm in length to which is attached a gas line or an oven for introducing the gaseous or solid exchange material. The canal region can be biased negatively with respect to the source at ground potential. The former configuration

permits the extraction of negative-ions which are created by the positive-ion beam from the exchange material itself [49]. Figure 20 shows a schematic drawing of the Oak Ridge-type source [3]. In this particular mode of operation the formation processes are not through charge exchange but volume processes. In the exchange mode (exchange canal at ground potential) use of universal-type, positive-ion sources permits generation of negative ions from any element which has a positive electron affinity as well as for metastable negative ions.

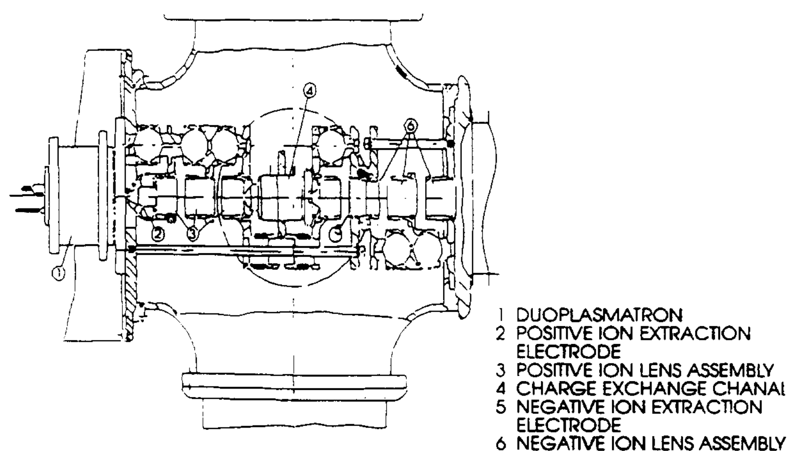

Fig. 20 Schematic drawing of a duoplasmatron charge exchange source at Oak Ridge.

4.3. Surface-Produced Negative Ion Sources

4.3.1. Sputter-type negative ion sources

Several versions of negative-ion sources are based on the fact that the yield of sputtered particles is greatly enhanced by the presence of a thin layer of cesium on the surface of the material being sputtered [50]. A schematic of one of the most versatile negative-ion sputter sources developed by Middleton and Adams is shown in Figure 21. The source uses a cesium-surface ionization source at ground potential. A cesium beam of 0.1 to 1 mA is accelerated to ≈ 20 keV and strikes a conical surface ≈ 20° half angle. The cesium serves both for sputtering and as an electron donor in the formation of negative ions. The negative ions are extracted through an aperture in the end of the cone. The source is equipped with an externally-indexable wheel containing several samples, which permits rapid change of ion samples. With this source currents in the range from 1 to 10 μA can be achieved, depending on the species.

Figure 22 shows the so-called "inverted" sputter source developed by Middleton [51] An annular ioniser is used to generate the Cs^+ sputter ion beam, which is accelerated on to a spherical sputter target. The negative ions produced by the sputter process are extracted through a hole in the ioniser.

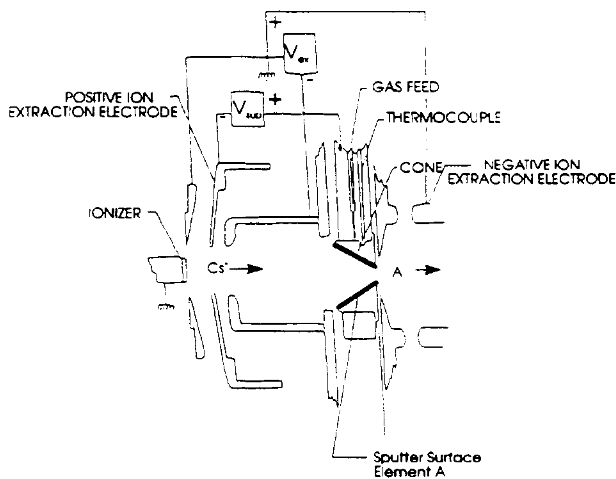

Fig. 21 Schematic drawing of the Middleton-Adams sputter source for negative ions

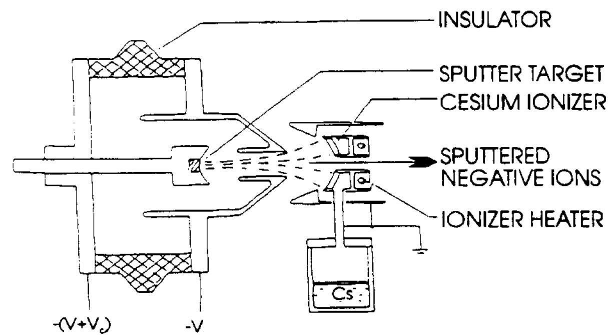

Fig. 22 "Inverted" Middleton sputter source for negative ions.

4.3.2. Plasma-surface-conversion negative-ion source

In the plasma-surface-conversion negative-ion sources the ions are formed at a negatively biased metal surface which is covered by cesium. The plasma forms a sheath in front of the sputter cathode which is negatively biased. Positive gas ions are accelerated and impinge on the surface. Negative gas ions formed at the surface are accelerated back across the plasma sheath toward the exit aperture. Cesium lowers the work function on the sputter cathode surface. Thereby the negative ion formation is strongly enhanced. This effect at cesiated surfaces was discovered in the magnetron source, where the conversion metal surface is the cathode itself [45], and adapted to Penning [52] and multi-cusp [53] sources where a separate converter/sputter-target is used. From a multi-cusp source of this type steady-state H^- beams of greater than 1 A [53] have been produced for fusion application.

Recently a new type of intense negative-ion source, based on plasma sputtering, has been developed at KEK [54] for negative ion production from solid materials. In this source the ions are produced from a metal surface negatively biased in a Xe plasma with Cs admixture (schematic see Fig. 23 [55]) confined by a cusp magnet field. The positive Xe/Cs ions sputter atoms, positive, and negative ions from the solid sputter material. Cesium atoms on the surface reduce the work function to less than 2 eV. For elements with a large electron affinity up to 10 % negative ion probability can be reached. In the first prototype of this source (Fig. 24) ion currents of 10 mA for Au^-, 10 mA for Cu^-, 6.4 mA for Pt^-, and 6 mA for Ni^- have been measured in pulsed mode (500 μs, 20 Hz) operation [55] . The 80 % normalized emittance of the 6 mA Ni^- beam was about 0.3 π mm mrad. The plasma was generated by hot filaments of LaB_6. More recent developments use microwave [55] or rf [56] plasma generation. These source types have now also developed for cw-operation. This is especially interesting for ion implantation, because the charge-up problem of ion-implanted insulators can be decreased.

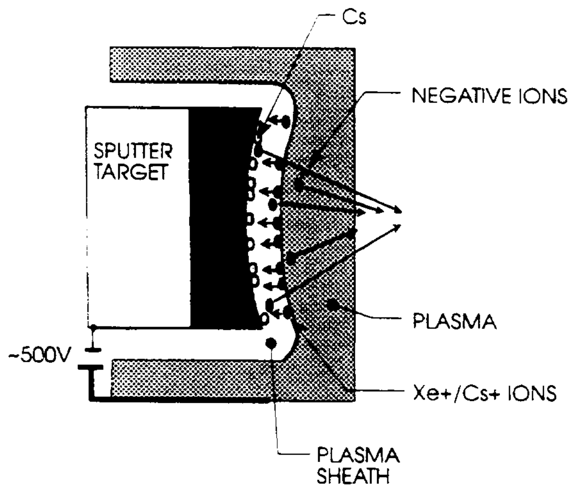

Fig. 23 Schematic of plasme sputter negative ion generation

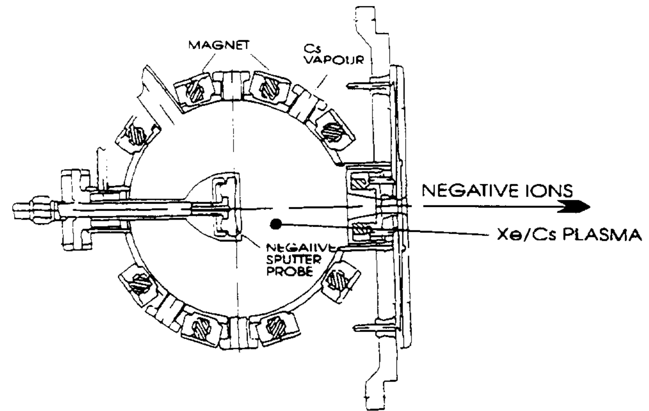

Fig. 24 KEK prototype of plasma sputter negative ion source

5. BEAM FORMATION

Most of the ion sources considered above are plasma sources, from which the ions are extracted through circular or slit apertures by applying a voltage. The principles of the ion optics involved are well known being similar to the optics of electron guns. New investigations have been stimulated by the development of high intensity beams for fusion application. Here only a few principles will be reviewed. The reader is referred to Ref. [57,58].

In a simple idealized model [57] (see Fig. 25) the ions are emitted from a curved plasma boundary, which establishes due to the balance between plasma pressure and the applied voltage. As a result the ions first converge toward this electrode. The ions then diverge as they pass through the aperture in the second electrode, this aperture being an electrostatic lens.

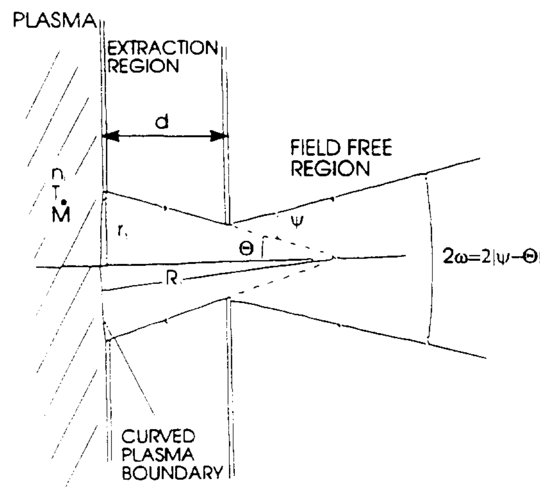

Fig. 25 Scheme of ion optics in beam extraction region.

The saturated ion current density J, which can be extracted from a plasma boundary is

$$J_s = n_i e \sqrt{\frac{kT_e}{M}} \quad (7)$$

Thus the total current I is

$$I = \pi r_1^2 J_s . \quad (8)$$

The current I [A] is related to the applied voltage U[V] by the equation

$$\frac{I}{U^{3/2}}\sqrt{\frac{M}{i}} = P_o \frac{A}{V^{3/2}} = 1.72 * 10^{-7}\left(\frac{r_1}{d}\right)^2 \quad (9)$$

where P_o is the perveance for plane parallel electrodes, M and I are the ion mass and charge respectively.

For a curved plasma boundary we can consider the current flow from a small circular area of a spherical surface. This results in a perveance of

$$P_s = P_0[1 - 1.6\, S\Theta] \quad (10)$$

where the aspect ratio $S = r_1/d$, and Θ as defined in Figure 25 is the convergence angle toward the extraction electrode. Taking into account the lens effect of the extractor the resulting beam divergence ω is given by

$$\omega = 0.29\, S\left(1 - 2.14\frac{P}{P_0}\right) \text{ rad.} \quad (11)$$

This equation predicts that $\omega = 0$ for $P = 0.47\ P_0$, or $\Theta \approx 0.6$ for $S \approx 1$, $\omega = 0$ is called the perveance matched condition and would be the optimum value for beam transmission. In practice, however, the divergence will not go to zero. This arises from optical aberations, from finite transverse ion energy (emittance) and from space-charge forces. One can also use Eq. (11) to relate the variation in divergence to the variation in perveance and hence in plasma density and obtain [58]

$$\Delta\omega = 16.6\, S\left(\frac{\Delta n_i}{n_i}\right) \text{ deg.} \quad (12)$$

This predicts that for $S = 1$ only ≈ 6 % variation in plasma density ($\approx$ plasma current) would change the divergence by 1°.

The most common designs of extraction systems use three electrodes (triodes). They consist of a beam-forming electrode, which defines the potential of the boundary of the plasma, an earth electrode and a suppressor electrode at a small negative potential which prevents electrons from backstreaming to the plasma source (see Fig. 26a).

Other systems in use are four-electrode systems (tetrodes) where a further electrode is inserted between the beam-forming electrode and the suppressor electrode (see Fig. 26b) to control the gradient of the electric field in the extraction gap. It is useful for changing both the beam optics and the electric stress in the electrode structure [59].

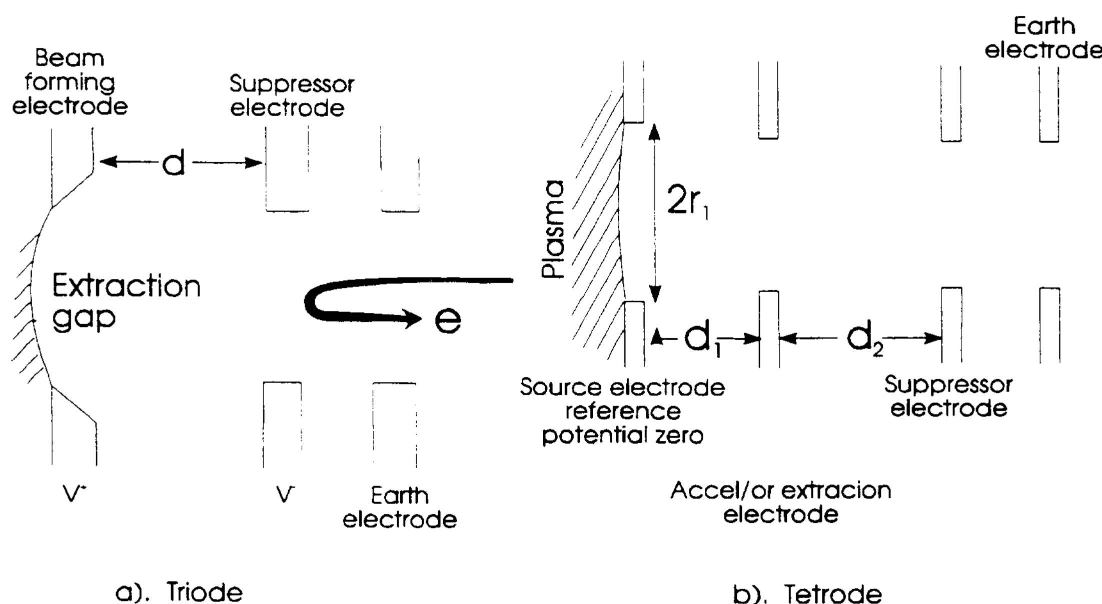

Fig. 26 Schematic drawings of commonly used acceleration electrode systems

Today extraction systems are mostly designed with the aid of computational methods for calculating the self-consistent electrical fields and particle trajectories. The major contributions of these methods in addition to the analytical treatments have been the accurate calculation of optimum perveance for special requirements such as maximum current or minimum divergence, and the detailed electrode design for both outlet and extractor electrodes [60].

REFERENCES

[1] H. Winter, B. Wolf, Plasma Physics 16, 791 (1974).

[2] J.M. Loiseaux, Nucl. Phys. A 354, 415 (1981).

[3] G.D. Alton, Proc. Int. Ion Engin. Congr., ISIAT '83, 85, (Kyoto 1983).

[4] H.W. Massay, Negative Ions, Ch.9, (Cambridge Univ. Press, London, 1976).

[5] B. Peart, K. Dolder, J. Phys. B: Atom. Molec. Phys. 8, 1570 (1975).

[6] R.J. Girnins, C.J. Anderson, L.W. Anderson, Phys. Rev. A 16, 2225 (1977).

[7] J. Heinemeier, P. Hvelplund, Nucl. Instr. & Meth. 148, 65 (1975).

[8] J. Heinemeier, P. Hvelplund, Nucl. Instr. & Meth. 148, 425 (1975).

[9] M. Kaminsky, Atomic and Ionic Impact Phenomena on Metal Surfaces (Springer Verlag, New York, 1965).

[10] V.E. Krohn, J. Appl. Phys. 33, 3523 (1962).

[11] J.D. Schneider et al., BNL-51134, 457 (Brookhaven 1979).

[12] R. Keller, Proc. 1984 Lin. Acc. Conf., GSI-84-11, 19 (1984).

[13] I.G. Brown, The Physics and Technology of Ion Sources, Ch. 7, 151, R. Keller, High-Current Gaseous Ion Sources, J. Wiley & Sons (1989).

[14] K.N. Leung, D.A. Bachmann, D.D. Mc Donald, Proc. 1992 Europ. Part. Acc. Conf., Berlin March 24-28, (1992).

[15] N. Sakudo, K. Tokiguchi, H. Koike, I. Kanomata, Rev. Sci. Instr. 48, 762 (1977).

[16] N. Sakudo, Microwave Ion Sources, in Ref. [13], Ch 11, p. 229.

[17] Y. Torii, M. Shimada, I. Watanabe, J. Hipple, C. Hayden, G. Dionne, Rev. Sci. Instr. 61, 253 (1990).

[18] T. Taylor, J.S.C. Wills, Nucl. Instr. Meth. A 309, 37 (1991).

[19] I.G. Brown, J.E. Galvin, B.F. Gavin, R.A. MacGill, Rev. Sci. Instr. 57, 1069 (1986).

[20] I.G. Brown, The Metal Vacuum Vapor Arc Ion Source, in Ref. [13], Ch 16, p. 331.

[21] I.G. Brown, M.R. Dickinson, J.E. Galvin, R.A. MacGill, Rev. Sci. Instr. 63, 2417 (1992).

[22] R.A. Demirkanov, H. Fröhlich, Proc. Int. Conf. on High-Energy. Acc., Brookhaven, p.224 (1962).

[23] C. Lejeune, Nucl. Instr. Meth. 116, 417 (1974).

[24] R. Keller, M. Müller, IEEE Trans. Nucl. Sci. NS-23, 1049 (1976).

[25] C. Bieth et al., IEEE Trans. Nucl. Sci. NS-19, 2 (1972).

[26] P.M. Mozorov et al., Atomnaya Energiya 3, 272 (1957).

[27] A.S. Pasyuk et al., Prib. Tekh. Eksp. 5, 23 (1963).

[28] E.D. Donets, IEEE Trans. Nucl. Sci. NS-23, 897 (1976).

[29] J. Arianer, R. Geller, Ann. Rev. Nucl. Part. Sci. 31, 19 (1981).

[30] J. Faure, Proc. 1984 Lin. Acc. Conf., GSI-84-11, p. 103, Darmstadt (1984).

[31] J. Faure, Proc. Int. Conf. on High-Energy Acc., Batavia p. 206 (1983).

[32] R. Becker, M. Kleinod, H. Klein, 2nd EBIS Workshop Saclay-Orsay (1981).

[33] T. Iwai et al., Phys. Rev. A 26, p. 105 (1982).

[34] E.D. Donets, Electron Beam Ion Sources, in Ref. [13], Ch 7, p. 245.

[35] A. Courtois, J. Faure, R. Gobin, P.A. Leroy, B. Visentin, P. Żupranski, Rev. Sci. Instr. 63, 2815 (1992).

[36] Y. Jongen, C.M. Lyneis, Electron Cyclotron Resonance Ion Sources, in Ref [13], Ch 10, p. 207.

[37] R. Geller, P. Ludwig, G. Melin, Ref. Sci. Instr. 63, 2795 (1992).

[38] M.P. Bourgarel, M. Bisch, J. Bony, P. Leherissier, J.Y. Pacquet, J.P. Rataud, Ch. Ricaud, Rev. Sci. Instr. 63, 2851 (1992).

[39] G. Melin et al., Rev. Sci. Instr. 61, 236 (1990).

[40] P. Sortais, Rev. Sci. Instr. 63, 2801 (1992).

[41] B.Yu. Sharkov, A.V. Shumshurov, V.B. Dubenkov, O.B. Sharmaev, A.A. Golubev, Rev. Sci. Instr. 63, 2841 (1992).

[42] T. Henkelmann, G. Korschinek, G. Belayev, V. Dubenkov, A. Golubev, S. Latyshev, B. Sharkov, A. Shumshurov, B. Wolf, Rev. Sci. Instr. 63, 2828 (1992).

[43] Y. Amdidouche, H. Haseroth, A. Kuttenberger, K. Langbein, J. Sellmair, T.R. Sherwood, B. Williams, B. Sharkov, O. Sharmaev, Rev. Sci. Instr. 63, 2838 (1992).

[44] K. Prelec, Th. Sluyters, Rev. Sci. Instr. 44, 1451 (1973).

[45] Yu.I. Belchenko, G.I Dimov, V.G. Dudnikov, Bull, Akad. Sci. USSR Phys. Ser. 39, 91 (1973).

[46] J.G. Alessi, Th. Slyuters, Rev. Sci. Instr. 51, 1630 (1980).

[47] K.N.Leung, C.A. Hauck, W.B.Kunkel, S.R. Walther, Rev. Sci. Instr. 60, 531 (1989).

[48] K.N. Leung, G.J. DeVries, W.F. DiVergilio, R.W. Hamm, C.A. Hauck, W.B. Kunkel, D.S. McDonald, M.D. Williams, Rev. Sci. Instr. 62, 100 (1991).

[49] W. Gentner, G. Hortig, Z. Phys. 172, 357 (1963).

[50] R. Middleton, C.T. Adams, Nucl. Instr. Meth. 118, 329 (1974).

[51] R. Middelton, IEEE Trans. Nucl. Sci. NS-23, 1098 (1976).

[52] K. Prelec, Nucl. Instr. Meth. 144, 413 (1977).

[53] K.N. Leung, K.W. Ehlers, Rev. Sci. Instr. 53, 803 (1982).

[54] G.D. Alton, Y. Mori, A. Takagi, A. Ueno, S. Fukumoto, Nucl. Instr. Meth. A 270, 194 (1988).

[55] Y. Mori, Rev. Sci. Instr. 63, 2357 (1992).

[56] J. Ishikawa, Rev. Sci. Instr. 63, 2368 (1992).

[57] J.R. Coupland, R.S. Green, D.P. Hammond, A.C. Riviere, Rev. Sci. Instr. 44, 1258 (1973).

[58] E. Thompson, Physica 104c, 199 (1981).

[59] T.S. Green, ISIAT '83 & IPAT '83, p. 13 (Kyoto 1983).

[60] P. Spädtke, GSI Int. Rep., GSI-83-9 (Darmstadt 1983).